Metabolic engineering of *Corynebacterium glutamicum* for the production of pyrone and pyridine dicarboxylic acids

Jae Sung Cho[a,b,1], Zi Wei Luo[a,b,1], Cheon Woo Moon[a,b,1], Cindy Pricilia Surya Prabowo[a,b], and Sang Yup Lee[a,b,c,2]

Significance

Exploration into alternative plastic monomers to replace petrochemical-derived monomers has been limited due to production challenges. One promising class of potential alternatives is pseudoaromatic compounds. This study presents the sustainable production of five pseudoaromatic dicarboxylic acids using metabolically engineered *Corynebacterium glutamicum* strains directly from glucose. A base production strain was constructed to produce 2-pyrone-4,6-dicarboxylic acid, which was then further engineered and optimized to produce other pyridine dicarboxylic acids. Fed-batch fermentation of the engineered strains demonstrated significant production titers. This work provides insight into the metabolic flexibility and engineering potential for synthesizing bio-based aromatic monomers using *C. glutamicum*. The methodologies from this study will be useful for developing efficient microbial cell factories to produce various bio-based plastic monomers.

Environmental concerns from plastic waste are driving interest in alternative monomers from bio-based sources. Pseudoaromatic dicarboxylic acids are promising alternatives with chemical structures similar to widely used petroleum-based aromatic dicarboxylic acids. However, their use in polyester synthesis has been limited due to production challenges. Here, we report the fermentative production of five pseudoaromatic dicarboxylic acids, including 2-pyrone-4,6-dicarboxylic acid (PDC) and pyridine dicarboxylic acids (PDCAs: 2,3-, 2,4-, 2,5-, and 2,6-PDCA), from glucose using five engineered *Corynebacterium glutamicum* strains. A platform *C. glutamicum* chassis strain was constructed by modulating the expression of nine genes involved in the synthesis and degradation pathways of precursor protocatechuate (PCA) and the glucose-uptake system. Comparative transcriptome analysis of the engineered strain against wild-type *C. glutamicum* identified *iolE* (*NCgl0160*) as a target for PDC production. Optimized fed-batch fermentation conditions enabled the final engineered strain to produce 76.17 ± 1.24 g/L of PDC. Using this platform strain, we constructed 2,3-, 2,4-, and 2,5-PDCA-producing strains by modulating the expression of key enzymes. Additionally, we demonstrated a previously uncharacterized pathway for 2,3-PDCA biosynthesis. The engineered strains produced 2.79 ± 0.005 g/L of 2,3-PDCA, 494.26 ± 2.61 mg/L of 2,4-PDCA, and 1.42 ± 0.02 g/L of 2,5-PDCA through fed-batch fermentation. To complete the portfolio, we introduced the 2,6-PDCA

biosynthetic pathway to an L-aspartate pathway–enhanced *C. glutamicum* strain, producing 15.01 ± 0.03 g/L of 2,6-PDCA in fed-batch fermentation. The metabolic engineering strategies developed here will be useful for the production of pseudoaromatic chemicals.

Corynebacterium glutamicum │ systems metabolic engineering │ pseudoaromatic dicarboxylic acid │ fed-batch fermentation │ sustainability

[a]Metabolic and Biomolecular Engineering National Research Laboratory, Department of Chemical and Biomolecular Engineering (BK21 Four Program), Korea Advanced Institute of Science and Technology, Daejeon 34141, Republic of Korea
[b]BioProcess Engineering Research Center, Korea Advanced Institute of Science and Technology, Daejeon 34141, Republic of Korea
[c]Graduate School of Engineering Biology, Korea Advanced Institute of Science and Technology, Daejeon 34141, Republic of Korea

The worldwide plastic production is estimated to be 1.1 billion tons by 2050 (1), while over 400 million tons of plastic waste are produced yearly with poor recycling rates, contributing significantly to global pollution in both marine and terrestrial environments (1–3). Urgent action is required to address this critical issue by reducing plastic waste, improving waste plastic recyclability, and shifting toward renewable resource-based bioplastics. A key focus within this transition is the search for environmentally friendly alternatives to the nonbiodegradable, petrochemical-derived terephthalic and isophthalic acids that form the backbone of many polymers (4, 5). Pseudoaromatic dicarboxylic acids are potential alternatives that exhibit structural similarity with aromatic dicarboxylic acids (Fig. 1*A*), demonstrating their polymerizable properties while maintaining biodegradability (4–6). Among the pseudoaromatic dicarboxylic acids, 2-pyrone-4,6-dicarboxylic acid (PDC) and pyridine dicarboxylic acids (PDCAs, i.e., 2,3-, 2,4-, 2,5-, and 2,6-PDCA) have recently garnered much attention as promising alternatives (3, 5, 7, 8).
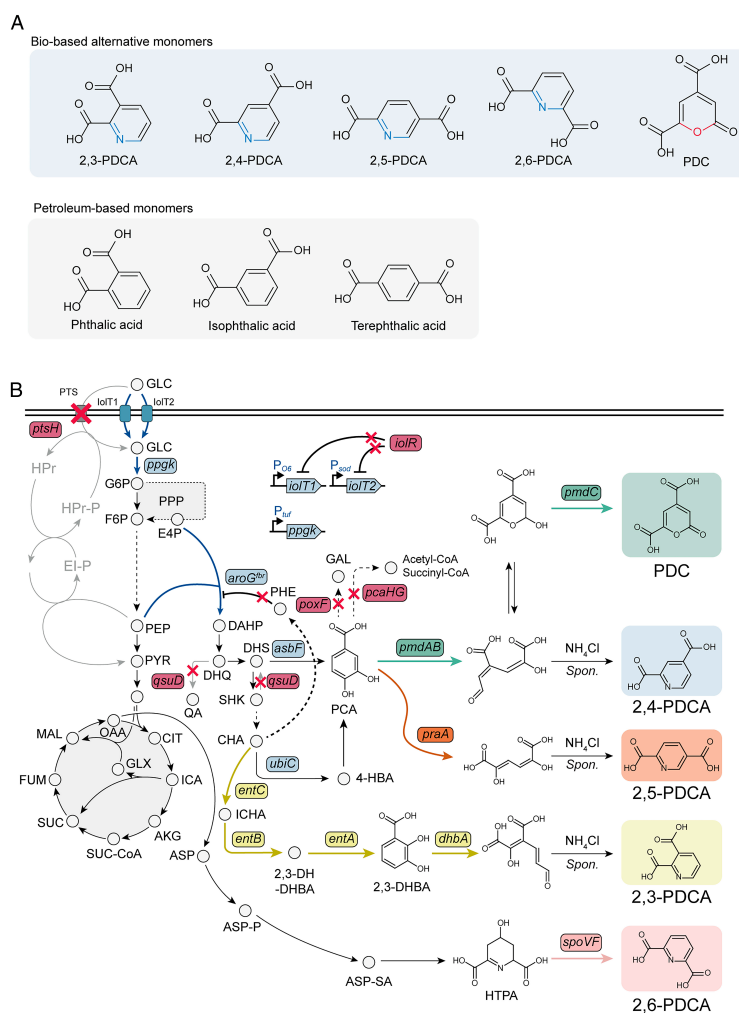
Fig. 1. Overview of pseudoaromatic dicarboxylic acid production using metabolically engineered *C. glutamicum*. (*A*) Structures of pseudoaromatic dicarboxylic acids and petroleum-derived aromatic dicarboxylic acids. (*B*) The metabolic network and metabolic engineering strategies employed for the production of pseudoaromatic dicarboxylic acids from glucose in *C. glutamicum*. Abbreviations and genes are detailed in *SI Appendix, Note S1*. Solid arrows indicate single metabolic reactions, while dashed arrows indicate multiple reactions. Overexpressed genes are marked in blue, and red Xs indicate gene deletions. *Spon.* denotes spontaneous reactions. The genes used for producing each pseudoaromatic dicarboxylic acid are marked in the same color as the background color of the corresponding pseudoaromatic dicarboxylic acid.

Pseudoaromatic dicarboxylic acids show considerable promise as monomers for biopolymers, yet their exploration has been limited, primarily due to synthesis challenges (*SI Appendix,* Fig. S1*A*). There have been few attempts to chemically produce PDCAs, and no known chemical method exists for producing PDC. PDCAs can be produced from *N*-heterocyclic compounds through strong oxidation (9–11) or a carbamoylation reaction followed by alkaline hydrolysis (12). However, most proposed chemical synthesis routes are challenging and impractical to commercialize due to low yield and selectivity, process complexity requiring multiple constrained catalytic steps (*SI Appendix,* Fig. S1*A*), precursor availability, and harsh reaction conditions posing environmental risks. Each chemical would need a specific production pipeline. In contrast, biological modalities for chemical production are inherently flexible, enabling the production of various pseudoaromatic dicarboxylic acids by modifying only a few genes or enzymatic steps. Engineered biological systems can produce the respective pseudoaromatic dicarboxylic acids from the same substrate (e.g., glucose) through fermentation under mild conditions (*SI Appendix,* Fig. S1*B*). Consequently, the versatility and sustainability of biological production for synthesizing pseudoaromatic dicarboxylic acids offer a promising approach to overcoming the challenges inherent in chemical methods.

PDC is naturally produced as a by-product in the microbial degradation of lignin-derived aromatic compounds by *Sphingomonas paucimobilis* SYK-6. Owing to its structural similarities to terephthalic acid, a key chemical precursor in the synthesis of various polymers including polyethylene terephthalate (PET), PDC has emerged to be a promising monomer, suitable for polymerizing with chemicals in a manner similar to terephthalic acid. This adaptability allows PDC to react with various diols and hydroxy acids, leading to the generation of various polymers such as PET-like (6, 13) and polybutylene terephthalate (PBT)-like polymers (14). The presence of the pseudoaromatic ring in PDC enables the PDC-based polymers to have several advantages, increasing their thermal stability (4, 6, 13, 14), Young's modulus (4, 6), mechanical strength (4, 6), adhering properties (15), elasticity (4), and biodegradability (4, 6). However, the chemical synthesis of PDC remains a challenging task. PDC production has been demonstrated using engineered *Pseudomonas putida* from lignin-derived aromatic compounds (14, 16, 17) and by converting terephthalic acid from PET waste through a chemo-microbial hybrid process (18). Additionally, we and others have shown the production of PDC directly from glucose using metabolically engineered *Escherichia coli* (3, 19, 20). Advancements in bio-based PDC production are expected to significantly contribute to the establishment of a PDC-based polymer industry.

2,3-Pyridine dicarboxylic acid (2,3-PDCA), more widely known as the nicotine precursor quinolinic acid, can also be used as a building block for metal coordination polymers created by cross-linking ligands (i.e., monomers) with the aid of transition-metal ions (21). For example, 2,3-PDCA has been cross-linked with the aid of Bi (III) ions, resulting in a Bi (III) coordination polymer with antibacterial activity (22). The production of 2,3-PDCA has been demonstrated in engineered *E. coli* and *Saccharomyces cerevisiae* through the metabolic engineering of their native L-aspartate pathway and kynurenine pathway, respectively (23, 24).

Likewise, 2,4-pyridine dicarboxylic acid (2,4-PDCA), 2,5-pyridine dicarboxylic acid (2,5-PDCA), and their derivatives can be polymerized to produce bio-based polyesters resembling isophthalic acid- and terephthalic acid-based polymers (5, 7). Furthermore, 2,6-pyridine dicarboxylic acid (2,6-PDCA), also known as dipicolinic acid and found in the endospores of Gram-positive bacteria (25, 26), has diverse applications. These include use as biodegradable chelating agents, antioxidants, and antimicrobial agents, as well as components of renewable bio-based polyesters (27–29).

The production of 2,4- and 2,5-PDCA has been demonstrated using metabolically engineered *Rhodococcus jostii* RHA1 from lignin (30). Additionally, the production of 2,6-PDCA has been demonstrated in low titers using metabolically engineered *E. coli* (31), *P. putida* (32), and *Corynebacterium glutamicum* (28) from glucose. Developing a systematic approach for engineering a microbial chassis strain capable of producing all four PDCAs from glucose would represent a significant first step toward the industrial production of these important plastic alternative monomers.

To this end, we chose to engineer *C. glutamicum*, a strain renowned for its industrial use in chemical production, as a microbial host to produce PDC and PDCAs. *C. glutamicum* has traditionally been widely used for the industrial production of valuable amino acids such as L-lysine and L-glutamate due to its robustness in large-scale fermentation (33). More recently, advanced metabolic engineering tools have been extensively developed for *C. glutamicum* (34, 35). Engineered *C. glutamicum* strains for the high-level production of L-lysine and shikimate pathway-derived products have been reported (36–38), from which the intermediate metabolites for PDC and PDCAs can be derived. Moreover, *C. glutamicum* is generally more tolerant to aromatic chemicals (39) compared to other production strains such as *E. coli* (38), making it a suitable host for the production of pseudoaromatic dicarboxylic acids.

In this study, we report the development of metabolically engineered *C. glutamicum* strains capable of producing pseudoaromatic dicarboxylic acids directly from glucose (Fig. 1*B*). Initially, the PDC biosynthetic pathway was constructed and optimized. Metabolic engineering was employed to increase precursor availability, resulting in a high-performance PDC-producing chassis strain. Subsequently, fed-batch fermentation conditions were optimized to enhance cell growth and PDC production. Comparative transcriptome analysis identified 17 target genes, which were overexpressed to further boost PDC production. Using one of the *C. glutamicum* chassis strains engineered for PDC production, we introduced the biosynthetic pathways for 2,3-, 2,4-, and 2,5-PDCA to produce the corresponding pseudoaromatic compounds. Optimization of supplementation concentrations and gene expression levels was performed to achieve high yields of these compounds under the optimized fed-batch fermentation conditions. For the production of 2,6-PDCA, an L-aspartate biosynthetic pathway–enhanced *C. glutamicum* strain was engineered by introducing five genes to convert oxaloacetate to 2,6-PDCA, thereby streamlining the flux toward 2,6-PDCA. Finally, fed-batch fermentations of the best-producing strains for each pseudoaromatic compound were conducted to demonstrate their potential for producing these compounds from glucose.

Results

Constructing a PDC Biosynthetic Pathway. Unlike *E. coli*, wild-type *C. glutamicum* ATCC 13032 can naturally produce PCA, the direct precursor to PDC, as an intermediate metabolite in the shikimate pathway. We initially constructed a synthetic pathway to convert the intermediate metabolite PCA to PDC (19) by overexpressing the *pmdAB* and *pmdC* genes encoding protocatechuate (PCA) 4,5-dioxygenase and 4-carboxy-2-hydroxymuconate-6-semialdehyde (CHMS) dehydrogenase, respectively, from *Comamonas testosteroni* ATCC 11996 under a strong constitutive P_{H36} promoter on plasmid pP1 (Fig. 2*A* and *SI Appendix,* Fig. S2). In flask cultivation, the *C. glutamicum* ATCC 13032 strain harboring pP1 produced 0.15 ± 0.02 g/L of PDC from glucose (*SI Appendix,* Fig. S3).

Fig. 2. Metabolic engineering of a platform *C. glutamicum* strain for the production of PDC. (*A*) The metabolic network for the production of PDC from glucose, along with the metabolic engineering strategies employed to overproduce PDC in this study. (*B*) Production of PDC using the *C. glutamicum* ATCC 13032 strain harboring different plasmid variants. (*C*) Genome engineering of *C. glutamicum* and its effect on PCA and PDC production. (*D*) PDC production using several fermentation condition optimization strategies. CSL: Corn steep liquor. (*E*) PDC production by plasmid-based overexpression of predicted overexpression targets based on the comparative transcriptome analysis between the *C. glutamicum* ATCC 13032 and PSE6 strains. (*F*) Fed-batch fermentation of the PSE6 strain harboring plasmids pP3 and pP1-0160. Abbreviations and genes are detailed in *SI Appendix, Note S1*. Symbols are green, PDC (g/L); white, cell density (OD$_{600}$); gray, PCA (g/L); black arrow, induction time point. Solid arrows indicate single metabolic reactions, while dashed arrows indicate multiple reactions. Overexpressed genes are marked in blue, and red X's indicate gene deletions. Error bars in the flask cultivation result represent the mean and SD from triplicate experiments. Error bars in the fed-batch fermentation result represent SD of biological duplicates; however, some error bars may be difficult to discern due to minimal SD.

To enhance PDC production by increasing the precursor PCA, targets for overexpression of genes were examined. There are two metabolic pathways leading to the production of precursor PCA from dehydroshikimate (*SI Appendix,* Fig. S4). The first involves a single enzymatic step using dehydroshikimate dehydratase, encoded by *qsuB*, as found natively in *C. glutamicum*. The second pathway consists of a series of enzymatic steps involving key intermediates such as shikimate, chorismate, and 4-hydroxybenzoate. To increase the flux toward precursor PCA, the effects of overexpressing specific genes were examined.

First, the genes *aroG*^{S180F} encoding a feedback-inhibition resistant mutant of DAHP synthase and *ubiC* from *Providencia rustigianii* NCTC6933 encoding chorismate pyruvate lyase were chosen as targets for overexpression. We have previously shown that the overexpression of the *aroG*^{S180F} gene was critical for increasing metabolic flux toward the shikimate pathway from glucose (38). The chorismate pyruvate lyase encoded by the *ubiC* gene is responsible for

converting chorismate to 4-hydroxybenzoate, which can subsequently be converted to PCA by 4-hydroxybenzoate hydroxylase (*SI Appendix,* Fig. S4). The genes $aroG^{S180F}$ and $ubiC$ were cloned to be expressed in an orthogonal plasmid under the IPTG-inducible P_{tac} promoter.

Although *C. glutamicum* natively expresses $qsuB$ encoding dehydroshikimate dehydratase, we sought to assess the impact of overexpressing two dehydroshikimate dehydratase genes on PDC production. The *Bacillus thuringiensis* $asbF$ gene and the native *C. glutamicum* $qsuB$ gene were cloned downstream of $aroG^{S180F}$ to construct plasmids pP3 and pP4, respectively (*SI Appendix,* Fig. S2). In addition, pP2, a high-copy number version (40) of plasmid pP1 expressing the $pmdABC$ operon was constructed. The four plasmids, pP1, pP2, pP3, and pP4, were introduced into *C. glutamicum* in various combinations (pP1 with pP3 or pP4, pP2 with pP3 or pP4) to assess PDC production. Flask cultivation results showed that the *C. glutamicum* ATCC 13032 strain harboring plasmids pP1 and pP3 produced the highest titer of 5.34 ± 0.13 g/L PDC (Fig. 2B). Therefore, the combination of plasmids pP1 and pP3 was used for further experiments.

Increasing Precursor PCA Supply for PDC Production by Genetic Manipulation. With the overexpression targets fixed, we focused on manipulating native chromosomal genes to increase the supply of the key precursor PCA for PDC production. First, we examined competing pathways involved in PDC biosynthesis. In *C. glutamicum*, PCA can be degraded into 3-carboxy-*cis*, *cis*-muconate by protocatechuate 3,4-dioxygenase, encoded by the $pcaHG$ genes, and further converted to acetyl-CoA and succinyl-CoA (41). To prevent the degradation of PCA, the PSE1 strain was constructed with a deletion of the $pcaHG$ genes. This modified strain, harboring plasmids pP1 and pP3, improved the PDC production titer to 7.74 ± 1.42 g/L (Fig. 2C).

Two additional gene targets were selected to further eliminate competing pathways. The $qsuD$ gene, which encodes quinate/shikimate dehydrogenase, was deleted to prevent the conversion of 3-dehydroquinate to quinate in the shikimate pathway, constructing the PSE2 strain. Additionally, the $poxF$ gene, which encodes phenol hydroxylase that catalyzes the conversion of PCA to gallic acid, was deleted from the PSE2 strain to construct the PSE3 strain (*SI Appendix,* Table S1). The resulting PSE2 and PSE3 strains, both harboring plasmids pP1 and pP3, produced 9.49 ± 0.77 g/L and 8.98 ± 2.18 g/L of PDC, respectively (Fig. 2C). Final cell densities of the PSE2 and PSE3 strains were slightly decreased compared to wild-type *C. glutamicum* ATCC 13032, indicating the deletion of the $qsuD$ gene results in decreased cell growth while increasing the production of PDC (*SI Appendix,* Fig. S5).

Next, we examined the effect of optimizing the glucose uptake systems to increase the flux from glucose. In native *C. glutamicum*, glucose uptake is facilitated by both the phosphoenolpyruvate (PEP)-dependent phosphotransferase system (PTS) and the PTS-independent pathway (42, 43). Since PEP is an important intermediate metabolite in the shikimate pathway, we explored shifting toward the PTS-independent glucose uptake system to enhance the shikimate pathway. The promoters of the $iolT1$ and $iolT2$ genes encoding nonphosphorylating *myo*-inositol permeases, and the $ppgk$ gene encoding polyphosphate-dependent glucokinases, were exchanged with the strong promoters P_{O6}, P_{sod}, and P_{tuf}, respectively, and the constructed PSE4 strain, harboring plasmids pP1 and pP3, produced 9.11 ± 0.17 g/L of PDC (Fig. 2C). While the genetic manipulations did not yield a statistically significant increase in PDC production for the PSE2, PSE3, and PSE4 strains, we continued further engineering on the PSE4 strain. This decision was based on the reasoning that these alternations would likely benefit, rather than harm, PDC production in scaled-up fermentations.

To further shift glucose uptake toward the PTS-independent system and increase the intermediate metabolite PEP pool, we disrupted the PTS-dependent glucose uptake system by deleting the *ptsH* gene, which encodes the phosphocarrier protein HPr, to construct the PSE5 strain. However, the PDC production by the PSE5 strain harboring plasmids pP1 and pP3 drastically dropped to 4.83 ± 0.32 g/L (Fig. 2C). We reasoned that the low-level PDC production resulted from inefficient glucose uptake by the PTS-independent glucose uptake system. To address this, the *iolR* gene (44), encoding the repressor of *iolT1*, was deleted to further enhance the efficiency of the PTS-independent glucose uptake system. The resulting PSE6 strain harboring plasmids pP1 and pP3 produced 10.89 ± 0.25 g/L of PDC (Fig. 2C). Lastly, we examined the impact of deleting the *hdpA* gene which encodes dihydroxyacetone phosphatase on PDC production by disrupting the flux toward glycerol, thereby increasing glyceraldehyde 3-phosphate and dihydroxyacetone phosphate (DHAP), resulting in the PSE7 strain (*SI Appendix*, Fig. S6). The PSE7 strain harboring plasmids pP1 and pP3 demonstrated decreased PDC titers of 4.56 ± 0.09 g/L. The higher cell density obtained with the PSE7 strain suggests that deleting the *hdpA* gene may have disrupted carbon balance (*SI Appendix*, Fig. S5), directing more carbon flux toward the TCA cycle via DHAP accumulation, and away from PDC production. Consequently, the best-performing PSE6 strain harboring plasmids pP1 and pP3 was selected for further experiments.

Fed-Batch Fermentation Optimization for PDC Production. The fed-batch fermentation of the engineered strain PSE6 was conducted using a 5 L bioreactor to examine its PDC production performance. The PSE6 strain harboring plasmids pP1 and pP3 produced 29.10 g/L of PDC in 96 h, with a yield of 0.237 mol/mol glucose and a productivity of 0.303 g/L/h from glucose in a minimal medium (*SI Appendix*, Fig. S7A). Given that the PSE6 strain produced 10.89 ± 0.25 g/L in flask cultivation, it was clear that there was significant room for improvement in production performance. Several fermentation condition optimization strategies were subsequently employed.

First, the IPTG induction time was delayed by 12 h to alleviate the burden of gene overexpression from induction at the start of fermentation. When induced at 12 h instead of at the start, the strain produced 30.62 g/L of PDC, with an improved yield of 0.278 mol/mol glucose and productivity of 0.425 g/L/h, while cell growth reached OD_{600} of 129 (*SI Appendix*, Fig. S7B). Next, to further reduce cell stress from intermittent glucose depletion due to the DO-stat feeding strategy, a pulsed feeding strategy (*SI Appendix, Materials and Methods*) was adopted. This new fermentation condition allowed the cells to produce 32.86 g/L of PDC, with a reduced yield of 0.142 mol/mol glucose, productivity of 0.390 g/L/h, and drastically improved cell growth reaching OD_{600} of 227 (*SI Appendix*, Fig. S7C).

We then compared the effect of supplementing the fermentation medium with a feasible nitrogen source to enhance strain performance. Supplementation with 10 g/L of yeast extract in the fed-batch fermentation improved PDC production to 43.43 g/L, with a yield of 0.141 mol/mol glucose and productivity of 0.517 g/L/h (*SI Appendix*, Fig. S7D). Corn steep liquor (CSL), a by-product of the corn wet milling process and widely used as a relatively inexpensive nitrogen source in the bio-industry, was tested as another supplement and an alternative to the more expensive yeast extract. Supplementing 40 g/L of CSL in flask cultivation improved PDC production to 12.54 ± 0.11 g/L compared to 11.14 ± 0.52 g/L with 10 g/L of yeast extract (*SI Appendix*, Fig. S8). With the supplementation of 40 g/L of CSL in fed-batch fermentation medium, the production titer reached a maximum of 62.03 g/L, with a yield of 0.206 mol/mol glucose and productivity of 0.523 g/L/h (Fig. 2D and *SI Appendix*, Fig. S7E).

Identification of Engineering Targets by Comparative Transcriptome Analysis. To explore nonobvious targets for further metabolic engineering of the PSE6 strain, a comparative transcriptome analysis between the *C. glutamicum* ATCC 13032 and PSE6 strains was performed (*SI Appendix*, Fig. S9 *A* and *B* and Dataset S1). The mRNA expression levels of genes involved in the *myo*-inositol pathway were significantly higher in the PSE6 strain, as expected, since the *iolR* deletion relieves the repression of the *myo*-inositol catabolism operon (45). To harness the high mRNA expression levels of *myo*-inositol catabolism genes, we sequentially deleted the *iol2* gene cluster (46) and the *iolW* gene to divert the metabolic flux toward cell growth. However, the engineered strains (PSE8 and PSE9) produced only 10.01 ± 0.12 g/L and 8.90 ± 0.94 g/L of PDC, respectively, showing a reduction in PDC production (*SI Appendix*, Fig. S9 *C* and *D*). This reduction in PDC production is consistent with deleting the *hdpA* gene to increase DHAP in the PSE7 strain (Fig. 2*C*).

Instead, we overexpressed the genes with significantly higher expression levels (>50-fold) to assess their impact on PDC production. Seventeen target genes were selected, excluding the previously engineered genes, and each target gene was overexpressed under the P_{H36} promoter in plasmid pP1, resulting in the construction of 17 plasmids (*SI Appendix*, Table S4). Each constructed plasmid was introduced into the PSE6 strain harboring plasmid pP3 to assess its effect on PDC production. Among the 17 strains, the PSE6 strain harboring plasmid pP3 and overexpressing *iolE* (*NCgl0160*) or *NCgl0552* in the plasmid pP1 (pP1-0160 or pP1-0552) produced 12.53 ± 0.20 and 12.19 ± 0.48 g/L of PDC, respectively. Interestingly, the simultaneous overexpression of the two genes, *iolE,* and *NCgl0552*, resulted in only 1.78 ± 1.01 g/L of PDC with observed growth retardation (Fig. 2*E* and *SI Appendix*, Fig. S10).

Fed-batch fermentations were conducted to further assess the production performance. The PSE6 strain harboring plasmids pP3 and pP1-0160 produced 76.17 ± 1.24 g/L of PDC with a yield of 0.36 ± 0.04 mol/mol glucose and a productivity of 0.63 ± 0.01 g/L/h (Fig. 2*F* and *SI Appendix*, Fig. S11*A*). The PSE6 strain harboring plasmids pP3 and pP1-0552 produced 67.41 g/L of PDC with a yield of 0.284 mol/mol glucose and a productivity of 1.12 g/L/h (*SI Appendix*, Fig. S11*B*). No precursor PCA was detected in either strain. Understanding how the overexpression of each of these two nonobvious target genes individually contributes to the increase in PDC production will be valuable for future studies. Leveraging transcriptome data to overexpress genes provides a valuable approach for identifying and enhancing nonobvious gene targets, which are otherwise challenging to discover through rational approaches only.

Construction of 2,3-, 2,4-, 2,5-PDCA Biosynthetic Pathways. The biosynthetic pathways for the production of 2,3-, 2,4-, and 2,5-PDCA are shown in Fig. 1*B*. The production of 2,4- and 2,5-PDCA from PCA involves two steps: the ring-cleavage of PCA by protocatechuate dioxygenase and the cyclization of the ring-opened product induced by ammonia (Fig. 3*A*) (7, 47). For the biosynthesis of 2,4- and 2,5-PDCA, the *ligAB* operon encoding protocatechuate 4,5-dioxygenase from *S. paucimobilis* SYK-6 and the *praA* gene encoding protocatechuate 2,3-dioxygenase from *Paenibacillus* sp. JJ-1b have been previously reported to catalyze the ring-cleavage reaction of PCA, respectively (47).
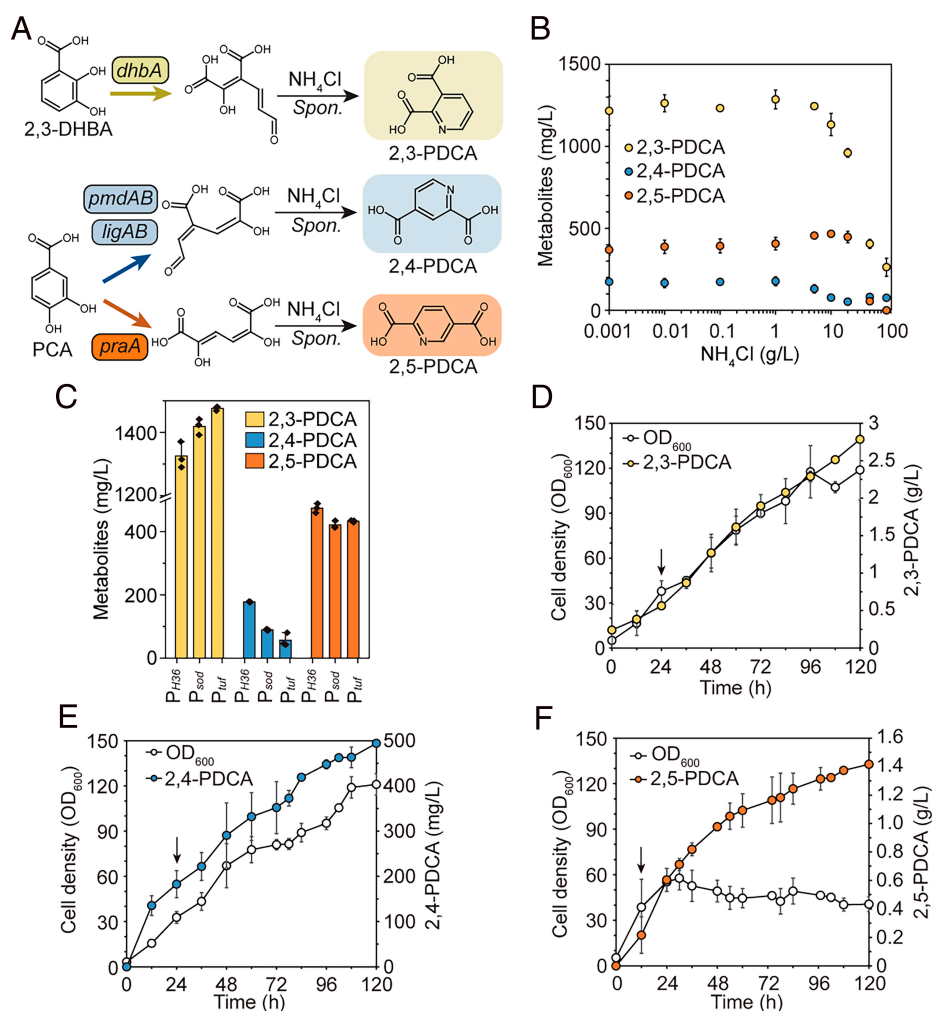
Fig. 3. Production of 2,3-, 2,4-, and 2,5-PDCA in engineered *C. glutamicum* strains. (*A*) Scheme of downstream conversion from PCA to 2,4-PDCA and 2,5-PDCA, and from 2,3-DHBA to 2,3-PDCA. (*B*) Effect of supplementary NH$_4$Cl concentration on the production of 2,3-, 2,4-, and 2,5-PDCA in flask cultivation using glucose as carbon source. (*C*) Effect of various promoters driving the optimization of the ring cleavage enzyme coding genes on the production of 2,3-, 2,4-, and 2,5-PDCA. (*D*) Fed-batch fermentation of the PSE10 strain harboring plasmids p23P3 and p23P1T. (*E*) Fed-batch fermentation of the PSE6 strain harboring plasmids pP3 and p24P2. (*F*) Fed-batch fermentation of the PSE6 strain harboring plasmids pP3 and p25P1. Genes are detailed in *SI Appendix, Note S1*. Notations: *Spon.*, spontaneous; yellow, 2,3-PDCA; blue, 2,4-PDCA; orange, 2,5-PDCA; white circle, cell density (OD$_{600}$); black arrow, induction time point. Error bars in the flask cultivation result represent the mean and the SD from triplicate experiments. Error bars in the fed-batch fermentation result represent SD of biological duplicates; however, some error bars may be difficult to discern due to the minimal SD.

We tested two genes encoding protocatechuate 4,5-dioxygenase: *pmdAB* from *C. testosteroni* ATCC 11996 and *ligAB* from *S. paucimobilis* SYK-6 to assess the 2,4-PDCA production performance. Plasmids p24P1, p24P2, and p25P1 were constructed to overexpress the *pmdAB*, *C. glutamicum* codon-optimized *ligAB*, and *C. glutamicum* codon-optimized *praA* gene under the P$_{H36}$ promoter, respectively. NH$_4$Cl was used as the additional ammonium source for the cyclization of the ring-cleaved product (Fig. 3*A*). The *C. glutamicum* ATCC 13032 strain harboring plasmids p24P1, p24P2, and p25P1, along with the cointroduction of plasmid pP3, produced 87.83 ± 7.58 mg/L, 147.23 ± 18.11 mg/L of 2,4-PDCA, and 121.72 ± 22.12 mg/L of 2,5-PDCA in flask cultivation with the supplementation of 1 g/L NH$_4$Cl, respectively (*SI Appendix*, Fig. S12*A*).

The production of 2,3-PDCA had previously been demonstrated through the L-aspartate or kynurenine pathways (23, 24). Following the biosynthesis mechanism for 2,4- and 2,5-PDCA, we reasoned that a similar ring-opening and cyclization mechanism might work for the conversion of 2,3-dihydroxybenzoic acid (2,3-DHBA) to 2,3-PDCA via ammonia-induced ring closure. The

pathway for producing the precursor 2,3-DHBA from chorismate comprises three enzymatic steps using isochorismate synthase, isochorismatase, and 2,3-dihydro-2,3-DHBA dehydrogenase, encoded by the *entC, entB,* and *entA* genes from *E. coli* W3110, respectively (48). The ring-cleavage of 2,3-DHBA can be performed by 2,3-dihydroxybenzoate 3,4-dioxygenase, encoded by the *dhbA* gene, from *Pseudomonas reinekei* MT1 (49). The spontaneous cyclization to 2,3-PDCA may occur in the presence of ammonium (Fig. 3*A*).

Two plasmids were constructed: plasmid p23P3 containing the *aroG*^{S180F}, *entC, entB,* and *entA* genes driven by the strong P$_{tac}$ promoter to increase the metabolic flux to the shikimate pathway and the conversion of chorismate to 2,3-DHBA, and the plasmid p23P1 containing the overexpressed *C. glutamicum* codon-optimized *dhbA* gene under the P$_{H36}$ promoter. The *C. glutamicum* ATCC 13032 strain harboring plasmids p23P3 and p23P1 produced 691.31 ± 100.17 mg/L of 2,3-PDCA with the addition of 1 g/L NH$_4$Cl (*SI Appendix*, Fig. S12*A*). Thus, we successfully demonstrate the production of 2,3-PDCA via a previously uncharacterized biosynthetic pathway that mimics the production pathways of 2,4- and 2,5-PDCA.

Increasing 2,3-, 2,4-, 2,5-PDCA Production. To increase the production of 2,3-, 2,4-, and 2,5-PDCA, we adopted the PSE6 strain, where the shikimate pathway was strengthened for PDC production. Since the production of 2,3-DHBA requires chorismate as a key intermediate, the *qsuB* gene encoding 3-dehydroshikimate dehydratase was deleted in the PSE6 strain to increase the flux to chorismate, resulting in the construction of the PSE10 strain. To confirm the capability of the PSE6 and PSE10 strains to produce 2,3-, 2,4-, and 2,5-PDCA, we first assessed the production of the precursors PCA and 2,3-DHBA in fed-batch fermentation. The PSE6 strain harboring plasmid pP3 produced 51.57 g/L of PCA, while the PSE10 strain harboring plasmid p23P3 produced 10.20 g/L of 2,3-DHBA (*SI Appendix*, Fig. S13 *A and B*).

Next, we introduced plasmids overexpressing the genes encoding ring-cleavage enzymes into the constructed strains. The PSE10 strain harboring plasmids p23P3 and p23P1 produced 1,094.25 ± 205.54 mg/L of 2,3-PDCA, while the PSE6 strain harboring plasmids p24P2 or p25P1, along with cointroduction of plasmid pP3, produced 177.34 ± 11.27 mg/L of 2,4-PDCA and 410.63 ± 5.71 mg/L of 2,5-PDCA in flask cultivation with 1 g/L NH$_4$Cl supplementation (*SI Appendix*, Fig. S12*B*).

To further increase the production of 2,3-, 2,4-, and 2,5-PDCA from direct precursors, we focused on the downstream conversion comprising ring opening and spontaneous cyclization. Since an additional ammonium source is needed for the pyridine ring formation step, various concentrations of NH$_4$Cl were tested in flask cultivation. Among the tested concentrations, 1 g/L NH$_4$Cl was optimal for producing 1,285.77 ± 3.78 mg/L of 2,3-PDCA and 177.44 ± 27.32 mg/L of 2,4-PDCA, while 10 g/L NH4Cl was optimal for producing 466.06 ± 15.01 mg/L of 2,5-PDCA (Fig. 3*B*).

Moreover, under the optimal NH$_4$Cl concentrations, we tested three different strong constitutive promoters to optimize the expression of the ring-opening enzymes. Plasmids p23P1T, p24P2T, and p25P1T were constructed from plasmids p23P1, p24P2, and p25P1 by exchanging the P$_{H36}$ promoter with the P$_{tuf}$ promoter, and plasmids p23P1S, p24P2S, and p25P1S were constructed by exchanging the P$_{H36}$ promoter with the P$_{sod}$ promoter. Results showed that the P$_{tuf}$ promoter was the best for 2,3-PDCA production, yielding 1,475.87 ± 6.35 mg/L of 2,3-PDCA, while the P$_{H36}$ promoter was better for both 2,4- and 2,5-PDCA, producing 177.77 ± 1.24 mg/L of 2,4-PDCA and 474.43 ± 14.60 mg/L of 2,5-PDCA, respectively (Fig. 3*C*).

Furthermore, we tested whether more basic pH conditions would affect production performance, as previous studies indicated that CHMS cyclization can be influenced by pH (50). While we speculated that the ring-cleaved product might cyclize more efficiently at higher pH, the production of 2,3-, 2,4-, and 2,5-PDCA all decreased at higher pH levels (*SI Appendix*, Fig. S14).

Finally, fed-batch fermentations of the 2,3-, 2,4-, and 2,5-PDCA producing strains were performed with the optimal NH_4Cl concentrations: 1 g/L for 2,3- and 2,4-PDCA production and 10 g/L for 2,5-PDCA production. The PSE10 strain harboring plasmids p23P3 and p23P1T produced 2.79 ± 0.005 g/L of 2,3-PDCA with a yield of 0.02 ± 0.0003 mol/mol glucose and a productivity of 0.02 ± 0.00004 g/L/h. The PSE6 strain harboring plasmids pP3 and p24P2 produced 494.26 ± 2.61 mg/L of 2,4-PDCA with a yield of 4.67 ± 0.002 mmol/mol glucose and a productivity of 4.12 ± 0.02 mg/L/h. The PSE6 strain harboring plasmids pP3 and p25P1 produced 1.42 ± 0.02 g/L of 2,5-PDCA with a yield of 0.02 ± 0.0002 mol/mol glucose and a productivity of 0.01 ± 0.0002 g/L/h (Fig. 3 *D–F* and *SI Appendix*, Fig. S15).

These results represent the highest fermentative production of 2,4- and 2,5-PDCA from glucose and the first production of 2,3-PDCA using the alternative pathway, to the best of our knowledge. Given that the toxicity assay showed significant growth retardation in wild-type *C. glutamicum* ATCC 13032 even at 0.1 g/L of 2,3-, 2,4-, and 2,5-PDCA (*SI Appendix*, Fig. S16 *A–C*), the engineered strains demonstrated here have achieved production titers well above the product's toxic levels. Future engineering strategies to overproduce 2,3-, 2,4-, and 2,5-PDCA in *C. glutamicum* could focus on increasing product tolerance.

Construction and Optimization of the 2,6-PDCA Biosynthetic Pathway. The biosynthesis of 2,6-PDCA requires a single-step conversion from (2S, 4S)-4-hydroxy-2,3,4,5-tetrahydrodipicolinic acid (HTPA), an intermediate in the L-lysine biosynthetic pathway (Fig. 4A and *SI Appendix*, Fig. S17A) (28). To achieve this, we constructed a synthetic pathway by overexpressing the *spoVFA* and *spoVFB* genes, which encode the dipicolinic acid synthase *spoVF* operon (51), in an L-lysine overproducing *C. glutamicum* BE strain (52) to convert HTPA to 2,6-PDCA. Plasmid p26P1 was constructed to overexpress the *spoVFA* and *spoVFB* genes from *Bacillus subtilis* under the P_{H36} promoter. The *C. glutamicum* BE strain harboring plasmid p26P1 produced 0.76 ± 0.04 g/L of 2,6-PDCA in flask cultivation, along with 6.56 ± 0.13 g/L of L-lysine as a by-product (*SI Appendix*, Fig. S17B).
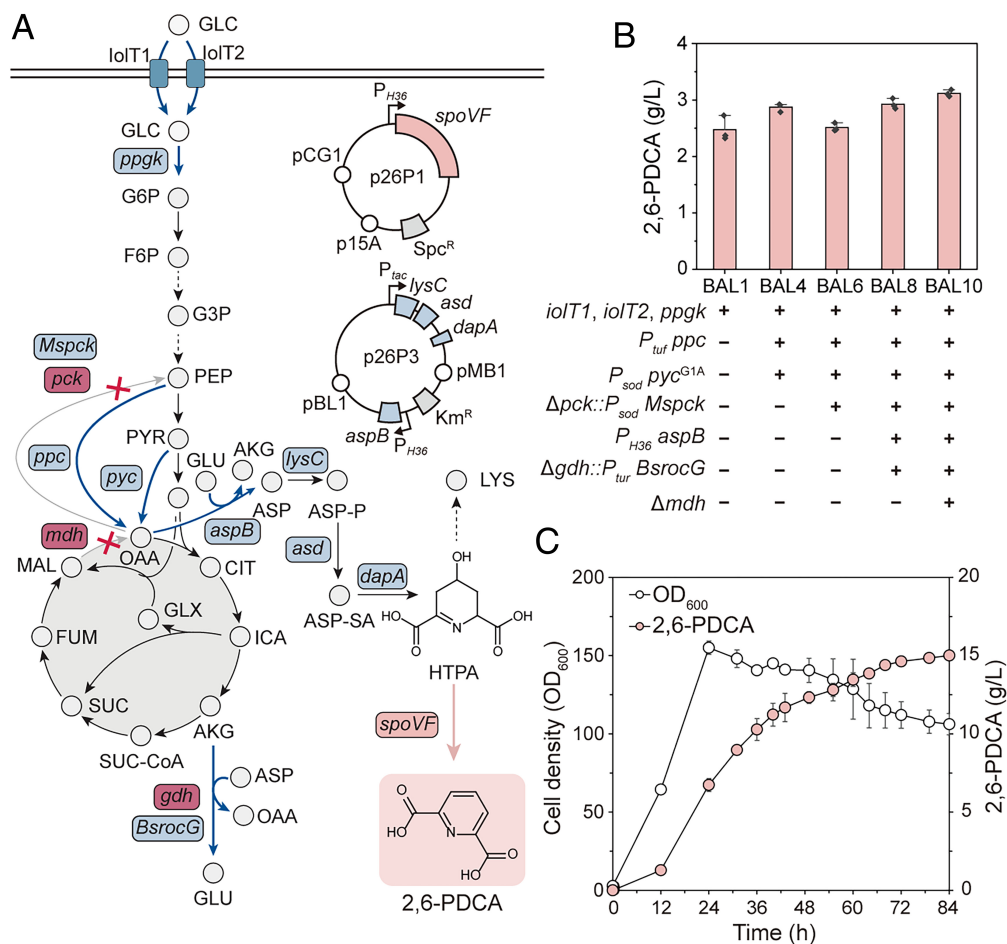
Fig. 4. Production of 2,6-PDCA in engineered *C. glutamicum*. (*A*) The metabolic network for the production of 2,6-PDCA from glucose as well as the metabolic engineering strategies employed in L-aspartate pathway-enhanced BAL strains. (*B*) The 2,6-PDCA production of the BAL strains harboring plasmids p26P1 and p26P3 in flask cultivation. (*C*) Fed-batch fermentation of the BAL10 strain harboring plasmids p26P1 and p26P3. Abbreviations and genes are detailed in *SI Appendix, Note S1*. Solid arrows indicate a single metabolic reaction, and dashed arrows indicate multiple reactions. Overexpressed genes are marked in blue, and red X's indicate gene deletions. Notations: Pink, 2,6-PDCA (g/L); white, cell density (OD$_{600}$). Error bars in the flask cultivation result represent the mean and the SD from triplicate experiments. Error bars in the fed-batch fermentation result represent SD of biological duplicates; however, some error bars may be difficult to discern due to the minimal SD.

	BAL1	BAL4	BAL6	BAL8	BAL10
iolT1, iolT2, ppgk	+	+	+	+	+
P$_{tuf}$ *ppc*	−	+	+	+	+
P$_{sod}$ *pyc*^{G1A}	−	+	+	+	+
Δ*pck*::P$_{sod}$ *Mspck*	−	−	+	+	+
P$_{H36}$ *aspB*	−	−	−	+	+
Δ*gdh*::P$_{tur}$ *BsrocG*	−	−	+	+	+
Δ*mdh*	−	−	−	−	+

To increase the precursor HTPA pool, we overexpressed three pathway genes to enhance the flux from L-aspartate to HTPA: the *lysC* gene encoding aspartokinase, the *asd* gene encoding aspartate semialdehyde dehydrogenase, and the *dapA* gene encoding dihydrodipicolinate synthase from *C. glutamicum*. These three genes were cloned to be expressed as an operon on an orthogonal plasmid under the IPTG-inducible P$_{tac}$ promoter, resulting in the construction of plasmid p26P2. The *C. glutamicum* BE strain harboring plasmids p26P2 and p26P1 produced 2.51 ± 0.19 g/L of 2,6-PDCA in flask cultivation, with 5.13 ± 0.19 g/L of L-lysine as a by-product (*SI Appendix*, Fig. S17*B*). Next, we overexpressed the *aspB* gene encoding L-aspartate aminotransferase under the P$_{H36}$ promoter in plasmid p26P2 to construct plasmid p26P3, aiming to increase the flux toward L-aspartate. The BE strain harboring plasmids p26P3 and p26P1 produced 2.97 ± 0.08 g/L of 2,6-PDCA and 4.08 ± 0.05 g/L of L-lysine in flask cultivation (*SI Appendix*, Fig. S17*B*).

Further Metabolic Engineering for Enhanced 2,6-PDCA Production. To further divert the metabolic flux toward 2,6-PDCA and reduce L-lysine production, we selected genome engineering target genes based on previous work done in *C. glutamicum* to overproduce L-lysine and its

derivatives (31, 36, 52). HTPA is an important intermediate in L-lysine biosynthesis and is also the direct precursor of 2,6-PDCA (*SI Appendix*, Fig. S17*A*).

First, we down-regulated the *dapB* gene, which encodes HTPA reductase, by changing its start codon from ATG to GTG to reduce the metabolic flux toward L-lysine and salvage the precursor HTPA, thereby constructing the PSE$_{BE}$1 strain. Next, we overexpressed the *ppc* gene, encoding phosphoenolpyruvate carboxylase, by replacing its native promoter with the P$_{H36}$ promoter to enhance the conversion of PEP to oxaloacetate, resulting in the construction of strain PSE$_{BE}$2. However, the PSE$_{BE}$1 and PSE$_{BE}$2 strains, harboring plasmids p26P1 and p26P3, exhibited severe growth retardation and reduced 2,6-PDCA production (*SI Appendix*, Fig. S18). Consequently, we shifted our strategy to manipulating the L-aspartate pathway without down-regulating the *dapB* gene. We deleted the *pck* gene, which encodes phosphoenolpyruvate carboxykinase, from the *C. glutamicum* BE strain to block the conversion of oxaloacetate to PEP and redirect the glycolytic flux toward HTPA, creating the PSE$_{BE}$3 strain. We also overexpressed the *ppc* gene by replacing its native promoter with the P$_{H36}$ promoter to construct the PSE$_{BE}$4 strain. To increase the NADPH used as a cofactor, we enhanced the pentose phosphate pathway by changing the promoter of the *tkt* gene encoding transketolase to the P$_{H36}$ promoter and altering the start codon of the *tkt* gene from TTG to ATG, resulting in the construction of the PSE$_{BE}$5 strain. Unfortunately, all constructed strains (PSE$_{BE}$3 through PSE$_{BE}$5), harboring plasmids p26P1 and p26P3, showed severe growth retardation and reduced 2,6-PDCA production (*SI Appendix*, Fig. S18). These results suggest that, although the L-lysine-producing *C. glutamicum* BE strain is efficient for the overproduction of L-lysine and its derivatives, redirecting the L-lysine biosynthetic pathway flux toward 2,6-PDCA in this strain is challenging.

Shifting away from the L-lysine-producing *C. glutamicum* BE strain, we leveraged L-aspartate pathway–enhanced *C. glutamicum* strains (BAL) we previously developed for β-alanine overproduction (42) as the chassis for 2,6-PDCA production. The BAL strains were constructed through gene expression manipulations of the PTS-independent glucose uptake system, the anaplerotic pathway, and the tricarboxylic acid (TCA) cycle. These modifications were guided by genome-scale metabolic simulations to enhance the metabolic flux toward L-aspartate.

We introduced plasmids p26P1 and p26P3 into the BAL strains and evaluated their 2,6-PDCA production capabilities. Notably, the strain BAL10, the best-performing strain for β-alanine production, also produced the highest amount (3.12 ± 0.06 g/L) of 2,6-PDCA in flask cultivation (Fig. 4*B*). Fed-batch fermentation of the best-performing strain BAL10 harboring plasmids p26P1 and p26P3 was conducted; however, cell growth retardation was observed when induced (*SI Appendix*, Fig. S19*A*). We reasoned that the growth retardation was due to the induction of genes and the toxicity of 2,6-PDCA, as the presence of 1 g/L of 2,6-PDCA in the medium completely suppressed the growth of the *C. glutamicum* ATCC 13032 strain (*SI Appendix*, Fig. S16*D*).

We then evaluated cell growth and 2,6-PDCA production of the BAL10 strain harboring only plasmid p26P1. This strain showed improved cell growth but decreased 2,6-PDCA production of 2.09 ± 0.18 g/L in flask cultivation (*SI Appendix*, Fig. S20), suggesting that optimal gene expression under the inducible promoter system in the second plasmid p26P3 can enable higher-level 2,6-PDCA production. To this end, we modulated IPTG concentrations to observe their effect on 2,6-PDCA production and cell growth in fed-batch fermentation. Additionally, to further reduce cell stress from intermittent glucose depletion arising from the pH-stat feeding strategy, a pulsed feeding strategy was implemented (*SI Appendix, Materials and Methods*).

Taken together, reducing the IPTG concentration to 10 μM alleviated growth retardation and increased 2,6-PDCA production (*SI Appendix*, Fig. S19 *B* and *C*). Moreover, completely omitting

IPTG induction to allow basal-level gene expression resulted in 2,6-PDCA production with minimal impact on cell growth (Fig. 4C and *SI Appendix*, Fig. S19*D*). Employing both the basal-level gene expression and pulsed feeding strategy enabled the BAL10 strain harboring plasmids p26P1 and p26P3 to achieve 2,6-PDCA production of 15.01 ± 0.03 g/L with a yield of 0.09 ± 0.001 mol/mol glucose and a productivity of 0.18 ± 0.0003 g/L/h, with less cell growth retardation observed (Fig. 4C and *SI Appendix*, Fig. S19*D*). To our knowledge, the concentration of 2,6-PDCA achieved is the highest value reported to date.

Discussion

In this paper, we developed five metabolically engineered *C. glutamicum* platform strains capable of producing pseudoaromatic dicarboxylic acids (PDC, 2,3-, 2,4-, 2,5-, and 2,6-PDCA) from glucose. A synthetic metabolic pathway toward PDC was constructed through the introduction of the *C. testosteroni pmdABC* operon (19). PDC production was optimized by the plasmid-based overexpression of the feedback-resistant $aroG^{S180F}$ gene, along with the *asbF* and *ubiC* genes, to increase the flux toward the precursor PCA. Genetic manipulation was performed to further increase the key precursor PCA supply by deleting the *pcaHG, qsuD*, and *poxF* genes, which are responsible for the competing pathways toward PCA biosynthesis, and by shifting the native glucose uptake system to use the PTS-independent glucose uptake system. This was achieved through promoter exchange of the *iolT1*, *iolT2*, and *ppgk* genes, and the deletion of the *ptsH* and *iolR* genes. Additionally, fed-batch fermentation conditions were optimized, resulting in the production of 62.03 g/L of PDC. Comparative transcriptome analysis led to the further overexpression of highly expressed genes (>50-fold) to assess their impact on PDC overproduction. Among 17 target genes, the PSE6 strain harboring plasmids pP3 and pP1-0160 produced 76.17 ± 1.24 g/L of PDC with an overall productivity of 0.63 ± 0.01 g/L/h and a yield of 0.36 ± 0.04 mol/mol glucose in fed-batch fermentation.

The 2,3-, 2,4-, and 2,5-PDCA biosynthesis pathways were constructed, with the 2,3-PDCA route being a previously unreported biosynthetic pathway in this study. The two-step enzymatic conversions from their respective direct precursors were optimized in the high PDC-producing strain (PSE6) to achieve 2.79 ± 0.005 g/L of 2,3-PDCA, 494.26 ± 2.61 mg/L of 2,4-PDCA, and 1.42 ± 0.02 g/L of 2,5-PDCA in fed-batch fermentation, all of which were well above the product tolerance levels. To complete the portfolio of pseudoaromatic dicarboxylic acid production, L-lysine overproducing *C. glutamicum* BE strain and L-aspartate pathway–enhanced *C. glutamicum* BAL strains were engineered to produce 2,6-PDCA. Production of 2,6-PDCA in BAL10 strain was optimized by introducing four genes to increase the flux toward the precursor HTPA and by optimizing fed-batch fermentation conditions. The final engineered strain produced 15.01 ± 0.03 g/L of 2,6-PDCA in optimized fed-batch fermentation.

This study marks a pivotal step in the sustainable production of pseudoaromatic dicarboxylic acids using engineered *C. glutamicum*, establishing a foundation and showcasing the potential of *C. glutamicum* as a microbial platform for producing plastic monomer alternatives. Furthermore, the metabolic engineering strategies described here offer a blueprint for designing microbial cell factories capable of efficiently producing chemicals of interest, including the pseudoaromatic chemicals described in this paper.

Materials and Methods

All of the materials and methods used in this study are detailed in *SI Appendix, Materials and Methods*, including culture media, construction of plasmids, genome manipulation, toxicity test with

2,3-, 2,4-, 2,5-, 2,6-PDCA, flask cultivations, fed-batch fermentations, comparative transcriptome analysis, and analytical methods.

Construction of Plasmids and Strains, Flask Cultivation, Fed-Batch Fermentation, and Analysis. Strains and plasmids used in this study were constructed as detailed in *SI Appendix*. Genomic manipulation was conducted as described in *SI Appendix*. Flask cultivations were cultured in 300 mL baffled flasks containing 25 mL of the appropriate medium on a shaking incubator at 200 rpm and 30 °C for 54 h. Fed-batch fermentations of the engineered strains were performed in a 6.6-L jar fermenter containing 1.8 L of appropriate medium. The agitation speed was adjusted to maintain the set DO level. The feed solution was pumped in at a rate of 10.7 mL/min as described in *SI Appendix*. Cell density was monitored using an Ultraspec 3000 spectrophotometer. The concentration of glucose and metabolites in the cell culture was measured using high-performance liquid chromatography.

Other Methods. Methods including toxicity test, and comparative transcriptome analysis are described in *SI Appendix*, *Materials and Methods*.

Data, Materials, and Software Availability

All study data are included in the article and/or supporting information.

Author contributions: J.S.C., Z.W.L., C.W.M., and S.Y.L. designed research; J.S.C., Z.W.L., C.W.M., and C.P.S.P. performed research; J.S.C., Z.W.L., and C.W.M. analyzed data; and J.S.C., Z.W.L., C.W.M., and S.Y.L. wrote the paper.

Competing interests: We disclose that S.Y.L. and one of the reviewers, P.I.N., had co-authored an editorial (https://pubmed.ncbi.nlm.nih.gov/38801001/).

1. E. N. Kalali et al., A critical review of the current progress of plastic waste recycling technology in structural materials. *Curr. Opin. Green Sustain. Chem.* **40**, 100763 (2023). Crossref.
2. S. Ko, Y. J. Kwon, J. U. Lee, Y. P. Jeon, Preparation of synthetic graphite from waste PET plastic. *J. Ind. Eng. Chem.* **83**, 449–458 (2020). Crossref.
3. F. Wu et al., Metabolic engineering of *Escherichia coli* for high-level production of the biodegradable polyester monomer 2-pyrone-4,6-dicarboxylic acid. *Metab. Eng.* **83**, 52–60 (2024). Crossref. PubMed.
4. T. Michinobu et al., Fusible, elastic, and biodegradable polyesters of 2-pyrone-4,6-dicarboxylic acid (PDC). *Polym. J.* **41**, 1111–1116 (2009). Crossref.
5. A. Pellis et al., Enzymatic synthesis of lignin derivable pyridine based polyesters for the substitution of petroleum derived plastics. *Nat. Commun.* **10**, 1762 (2019). Crossref. PubMed.
6. T. Michinobu et al., Polyesters of 2-pyrone-4,6-dicarboxylic acid (PDC) obtained from a metabolic intermediate of lignin. *Polym. J.* **40**, 68–75 (2008). Crossref.
7. C. W. Johnson et al., Innovative chemicals and materials from bacterial aromatic catabolic pathways. *Joule.* **3**, 1523–1537 (2019). Crossref.
8. M. G. Vasquez-Ríos, I. Rojas-León, P. Montes-Tolentino, I. F. Hernández-Ahuactzi, H. Höpfl, Pyridinedicarboxylic acids as versatile building blocks for coordination-driven self-assembly: Solvent-induced macrocycle and coordination polymer formation upon combination of 2,5-pyridinedicarboxylate with diorganotin moieties. *Cryst. Growth Des.* **18**, 7132–7149 (2018). Crossref.
9. G. Ghelli, E. Bruschi, G. Agnese, "Two stage process for preparing 2,6-pyridinedicarboxylic acid" US4419515A (1983).
10. W. Orth, E. Pastorek, W. Fickert, "Oxidation of quinoline to quinolinic acid" US4549024A (1985).
11. J. Toomey Jr., "Electrochemical oxidation of pyridine bases" US4482439 (1984).

12. J.-P. Roduit, A. Wellig, K. Amacker, M. Eyer, "Process for the preparation of 2, 4-pyridine dicarboxylic acid" US5614636A (1997).

13. T. Michinobu et al., Synthesis and characterization of hybrid biopolymers of L-lactic acid and 2-pyrone-4,6-dicarboxylic acid. *J. Macromol. Sci. A.* **47**, 564–570 (2010). Crossref.

14. S. Lee et al., Microbial production of 2-pyrone-4,6-dicarboxylic acid from lignin derivatives in an engineered *Pseudomonas putida* and its application for the synthesis of bio-based polyester. *Bioresour. Technol.* **352**, 127106 (2022). Crossref. PubMed.

15. M. Hishida et al., Polyesters of 2-pyrone-4, 6-dicarboxylic acid (PDC) as bio-based plastics exhibiting strong adhering properties. *Polym. J.* **41**, 297–302 (2009). Crossref.

16. Y. Otsuka et al., High-level production of 2-pyrone-4,6-dicarboxylic acid from vanillic acid as a lignin-related aromatic compound by metabolically engineered fermentation to realize industrial valorization processes of lignin. *Bioresource. Technol.* **377**, 128956 (2023). Crossref. PubMed.

17. Y. Otsuka et al., Efficient production of 2-pyrone 4,6-dicarboxylic acid as a novel polymer-based material from protocatechuate by microbial function. *Appl. Microbiol. Biotechnol.* **71**, 608–614 (2006). Crossref. PubMed.

18. M. J. Kang et al., A chemo-microbial hybrid process for the production of 2-pyrone-4,6-dicarboxylic acid as a promising bioplastic monomer from PET waste. *Green Chem.* **22**, 3461–3469 (2020). Crossref.

19. Z. W. Luo, W. J. Kim, S. Y. Lee, Metabolic engineering of *Escherichia coli* for efficient production of 2-pyrone-4,6-dicarboxylic acid from glucose. *ACS Synth. Biol.* **7**, 2296–2307 (2018). Crossref. PubMed.

20. D. Zhou et al., Multi-step biosynthesis of the biodegradable polyester monomer 2-pyrone-4, 6-dicarboxylic acid from glucose. *Biotechnol. Biofuels Bioprod.* **16**, 92 (2023). Crossref. PubMed.

21. S. Kitagawa, R. Kitaura, S. I. Noro, Functional porous coordination polymers. *Angew. Chem. Int. Ed. Engl.* **43**, 2334–2375 (2004). Crossref. PubMed.

22. M. Kowalik et al., Structural insights into new Bi(III) coordination polymers with pyridine-2, 3-dicarboxylic acid: Photoluminescence properties and anti-*Helicobacter pylori* activity. *Int. J. Mol. Sci.* **21**, 8696 (2020). Crossref. PubMed.

23. K. Ohashi, S. Kawai, K. Murata, Secretion of quinolinic acid, an intermediate in the kynurenine pathway, for utilization in NAD+ biosynthesis in the yeast *Saccharomyces cerevisiae*. *Eukaryot. Cell* **12**, 648–653 (2013). Crossref. PubMed.

24. F. Zhu, M. Pena, G. N. Bennett, Metabolic engineering of *Escherichia coli* for quinolinic acid production by assembling L-aspartate oxidase and quinolinate synthase as an enzyme complex. *Metab. Eng.* **67**, 164–172 (2021). Crossref. PubMed.

25. M. Paidhungat, K. Ragkousi, P. Setlow, Genetic requirements for induction of germination of spores of *Bacillus subtilis* by Ca(2+)-dipicolinate. *J. Bacteriol.* **183**, 4886–4893 (2001). Crossref. PubMed.

26. T. A. Slieman, W. L. Nicholson, Role of dipicolinic acid in survival of *Bacillus subtilis* spores exposed to artificial and solar UV radiation. *Appl. Environ. Microbiol.* **67**, 1274–1279 (2001). Crossref. PubMed.

27. C. P. Roupakias, G. Z. Papageorgiou, G. P. Karayannidis, Synthesis and thermal behavior of polyesters derived from 1,3-propanediol and various aromatic dicarboxylic acids. *J. Macromol. Sci. Part A: Pure Appl. Chem.* **40**, 791–805 (2003). Crossref.

28. L. S. Schwardmann, A. K. Dransfeld, T. Schaffer, V. F. Wendisch, Metabolic engineering of *Corynebacterium glutamicum* for sustainable production of the aromatic dicarboxylic acid dipicolinic acid. *Microorganisms* **10**, 730 (2022). Crossref. PubMed.

29. F. Takahashi, N. Sumitomo, H. Hagihara, K. Ozaki, Increased dipicolinic acid production with an enhanced *spoVF* operon in *Bacillus subtilis* and medium optimization. *Biosci. Biotechnol. Biochem.* **79**, 505–11 (2015). Crossref. PubMed.

30. E. M. Spence, L. Calvo-Bado, P. Mines, T. D. H. Bugg, Metabolic engineering of *Rhodococcus jostii* RHA1 for production of pyridine-dicarboxylic acids from lignin. *Microb. Cell Fact.* **20**, 15 (2021). Crossref. PubMed.

31. M. K. McClintock, G. W. Fahnhorst, T. R. Hoye, K. Zhang, Engineering the production of dipicolinic acid in *E. coli*. *Metab. Eng.* **48**, 208–217 (2018). Crossref. PubMed.

32. Y. Wang, J. Zheng, Y. Xue, B. Yu, Engineering *Pseudomonas putida* KT2440 for dipicolinate production via the entner-doudoroff pathway. *J. Agric. Food Chem.* **72**, 6500–6508 (2024). Crossref. PubMed.

33. J. Becker, C. Wittmann, Bio-based production of chemicals, materials and fuels -*Corynebacterium glutamicum* as versatile cell factory. *Curr. Opin. Biotechnol.* **23**, 631–640 (2012). Crossref. PubMed.

34. J. S. Cho et al., Targeted and high-throughput gene knockdown in diverse bacteria using synthetic sRNAs. *Nat. Commun.* **14**, 2359 (2023). Crossref. PubMed.

35. G. Y. Kim et al., Synthetic biology tools for engineering *Corynebacterium glutamicum*. *Comput. Struct. Biotechnol. J.* **21**, 1955–1965 (2023). Crossref. PubMed.

36. J. Becker, O. Zelder, S. Hafner, H. Schroder, C. Wittmann, From zero to hero–Design-based systems metabolic engineering of *Corynebacterium glutamicum* for L-lysine production. *Metab. Eng.* **13**, 159–168 (2011). Crossref.

PubMed.

37. N. Kallscheuer, J. Marienhagen, *Corynebacterium glutamicum* as platform for the production of hydroxybenzoic acids. *Microb. Cell Fact.* **17**, 70 (2018). Crossref. PubMed.

38. Z. W. Luo, J. S. Cho, S. Y. Lee, Microbial production of methyl anthranilate, a grape flavor compound. *Proc. Natl. Acad. Sci. U.S.A.* **116**, 10749–10756 (2019). Crossref. PubMed.

39. Y. B. Liu et al., Physiological roles of mycothiol in detoxification and tolerance to multiple poisonous chemicals in *Corynebacterium glutamicum*. *Arch. Microbiol.* **195**, 419–429 (2013). Crossref. PubMed.

40. J. W. Choi, S. S. Yim, K. J. Jeong, Development of a high-copy-number plasmid via adaptive laboratory evolution of *Corynebacterium glutamicum*. *Appl. Microbiol. Biotechnol.* **102**, 873–883 (2018). Crossref. PubMed.

41. X. Shen, S. Liu, Key enzymes of the protocatechuate branch of the beta-ketoadipate pathway for aromatic degradation in *Corynebacterium glutamicum*. *Sci. China Ser. C: Life Sci.* **48**, 241–249 (2005). PubMed.

42. M. R. Ghiffary, C. P. S. Prabowo, J. J. Adidjaja, S. Y. Lee, H. U. Kim, Systems metabolic engineering of *Corynebacterium glutamicum* for the efficient production of beta-alanine. *Metab. Eng.* **74**, 121–129 (2022). Crossref. PubMed.

43. S. N. Lindner, G. M. Seibold, A. Henrich, R. Kramer, V. F. Wendisch, Phosphotransferase system-independent glucose utilization in *Corynebacterium glutamicum* by inositol permeases and glucokinases. *Appl. Environ. Microbiol.* **77**, 3571–3581 (2011). Crossref. PubMed.

44. S. Klaffl, M. Brocker, J. Kalinowski, B. J. Eikmanns, M. Bott, Complex regulation of the phosphoenolpyruvate carboxykinase gene *pck* and characterization of its GntR-type regulator IolR as a repressor of *myo*-inositol utilization genes in *Corynebacterium glutamicum*. *J. Bacteriol.* **195**, 4283–4296 (2013). Crossref. PubMed.

45. T. Walter et al., Fermentative *N*-methylanthranilate production by engineered *Corynebacterium glutamicum*. *Microorganisms.* **8**, 866 (2020). Crossref. PubMed.

46. P. Ramp et al., Metabolic engineering of *Corynebacterium glutamicum* for production of *scyllo*-inositol, a drug candidate against Alzheimer's disease. *Metab. Eng.* **67**, 173–185 (2021). Crossref. PubMed.

47. Z. Mycroft, M. Gomis, P. Mines, P. Law, T. D. H. Bugg, Biocatalytic conversion of lignin to aromatic dicarboxylic acids in *Rhodococcus jostii* RHA1 by re-routing aromatic degradation pathways. *Green Chem.* **17**, 4974–4979 (2015). Crossref.

48. X. Sun, Y. Lin, Q. Yuan, Y. Yan, Biological production of muconic acid via a prokaryotic 2,3-dihydroxybenzoic acid decarboxylase. *Chemsuschem* **7**, 2478–2481 (2014). Crossref. PubMed.

49. M. Marin, I. Plumeier, D. H. Pieper, Degradation of 2,3-dihydroxybenzoate by a novel meta-cleavage pathway. *J. Bacteriol.* **194**, 3851–60 (2012). Crossref. PubMed.

50. H. Gómez-Alvarez et al., Bioconversion of lignin-derived aromatics into the building block pyridine 2,4-dicarboxylic acid by engineering recombinant *Pseudomonas putida* strains. *Bioresour. Technol.* **346**, 126638 (2022). Crossref. PubMed.

51. R. A. Daniel, J. Errington, Cloning, DNA sequence, functional analysis and transcriptional regulation of the genes encoding dipicolinic acid synthetase required for sporulation in *Bacillus subtilis*. *J. Mol. Biol.* **232**, 468–483 (1993). Crossref. PubMed.

52. T. Han, G. B. Kim, S. Y. Lee, Glutaric acid production by systems metabolic engineering of an l-lysine-overproducing *Corynebacterium glutamicum*. *Proc. Natl. Acad. Sci. U.S.A.* **117**, 30328–30334 (2020). Crossref. PubMed.